CSCE Annual Conference
Growing with youth – Croître avec les jeunes

Laval (Greater Montreal) June 12 - 15, 2019

NUMERICAL MODELLING OF NATURE-LIKE FISH PASSAGE USING A 2D SHALLOW WATER MODEL

Baki, A.B.[1,3], Golpira, A.[1], Rampinelli, G.C.[1], Patrizio, L.[1], Zhu, D.Z.[2]
[1]Clarkson University, Potsdam, New York, USA.
[2]University of Alberta, Edmonton, Canada.
[3]abaki@clarkson.edu

Abstract: Flow around fish habitat structures (e.g., boulders, rocks) is of great interest, particularly for fish passage technology. Modelling such three-dimensional (3D) complex hydraulics associated with habitat structure using an industrial 2D code solving Saint Venant equations may appear at first as a challenge. The purpose of this study is to determine the ability of a 2D code (River2D) to model flow through rock-ramp type nature-like fish pass and its limitations. The model was tested based upon the comparison between numerous experimental measurements and numerical simulations. The impact of varying computational mesh discretization and model calibration parameters on the accuracy of reproducing fish pass hydraulics was investigated using the River2D model. The results demonstrate that 2D shallow water model, River2D, model can be a convenient way for the hydraulic engineer to help design a nature-like fish pass.

1 INTRODUCTION

Hydraulic structures implemented in natural rivers, such as dams and weirs, cause several changes in native fish species' life cycle. These structures pose some difficulties for fish migrating upstream or downstream and limit their access to areas that are necessary for their life cycle (Katopodis et al. 2001). In this way, the changes in the streamflow velocity caused by these obstacles jeopardize the natural cycle of feeding and reproduction of several fish species. To mitigate the harmful effects of hydraulic barriers in fish's natural environments, fish transportation mechanisms (fishways or fish passages) have arisen as an alternative. A fish pass is defined as a waterway designed to allow the passage of fish species over obstructions in a natural streamflow (Puertas et al. 2012).

Traditionally, pool and weir fishways, that consist of a slanted channel that is divided by deflectors in a series of chambers (pools), are commonly used around the world (Clay 1995). Since each fish species have their own favorable hydraulic conditions to migration, several designs of the hydraulic characteristics of these facilities have been proposed to better fit the hydraulic configuration to attend a wide variety of species (Puertas et al. 2012). Significant efforts have been made to develop fish passages for different fish species (Williams et al. 2012). Some efforts were directed toward increasing fish passage efficiency (e.g., Roscoe and Hinch 2010; Noonan et al. 2012; Kim et al. 2016; Peter et al. 2017) while other studies investigated fish behavior (e.g., Hinch and Bratty 2000; Jones et al.1974; Sfakiotakis et al. 1999).

In recent years, a new concept of ecological or nature-like fish passage design named rock-ramp fish passage has emerged as a possibility of mimicking natural stream characteristics, providing suitable passage conditions for a wide variety of fish species (Baki et al. 2014). To investigate different characteristics of the rock-ramp fish passage and its hydraulics behaviour, some studies have been conducted recently (Baki, et al. 2014a; 2014b; 2016; 2017a; 2017b). Studies with comparisons between physical and numerical models of fish passages are an important approach to improve not only the knowledge about fish performance and fish passages design, but also the numerical modelling capabilities of reproducing the hydraulics of fishways accordingly. Accurate model predictions are important in echohydraulics because they are used to characterize and quantify the quality and extent of aquatic habitat in assessment, management, and restoration programmes (Ghamry and Katopodis 2017).

Since the hydraulics behind fishways is essentially a tridimensional phenomenon, the use of 3D turbulent flows models seems initially as the optimal models to effectively reproduce the complexity of the real flow through that structures. However, due to the input requirements, complex setting-up, and to excessive CPU time consumed by 3D free surface codes, there remains an interest for a 2D code. Hence, the use of 2D models may be an interesting strategy because they not only demand less input data and parameters than 3D models but also provide a minimum complexity unavailable in 1D models.

In this sense, the purpose of this paper is to determine the ability of a 2D code to model flow through a rock-ramp type nature-like fishpases and its limitations. This study aimed to investigate the performance of applying a River2D to reproduce depth-averaged velocity and water depth measured in a rock-ramp fish passage that was physically modeled in an experiment conducted by Baki et al. (2014a). Since the definition of the mesh resolution has a pronounced effect on the precision of simulating depth-averaged velocity and water depth (Ghamry and Katopodis 2017), the effect of using different spatial discretization was assessed first to define the optimal mesh size. Then, the most effective model calibration parameters that bring a model prediction into agreement with measured data was investigated.

2 MATERIALS AND METHODS

2.1 Model (River2D) development

The computational domain of the rock-ramp fish pass that was reproduced using the geometry of the flume used during the experimental study by Baki et al. (2014a), was about 9.0 m long, 0.92 m wide, and 0.61 m tall with a staggered arrangement of spherical isolated natural boulders (Figure 1). The boulders were arranged in 23 rows alternating between two and three boulders per row, resulting in a total of 11 cells (Figure 1). The bed slope of the rock-ramp fish pass was 5%. The water depth was measured along the channel center line between zones 5 and 7. The velocity was observed along the center and side center lines in zone 6 as shown in Figure 1. In the present paper measurements at flow rate of 60 L/s was only modelled. Details of the experimental setup and measurements are available in Baki et al. (2014a), who investigated the flow characteristics of rock-ramp to develop an integrated design procedure for rock-ramp fish passage.

A two-dimensional hydrodynamic model, River2D, developed specifically for use in natural streams and rivers (Steffler and Blackburn 2002), used in this study to conduct the numerical simulations. The River2D model uses the finite element method to solve the depth-integrated form of the Saint-Venant equations for conservation of mass and momentum (Steffler and Blackburn 2002). The model exterior boundaries were set at the upstream using flow rate and at the downstream setting observed water surface elevation. The isolated boulders were assumed as internal solid walls and the channel bed was modelled as a friction zone. Breaklines were applied at locations of significant topographic changes (e.g., boulders and steep banks) to aid in correct interpolation.

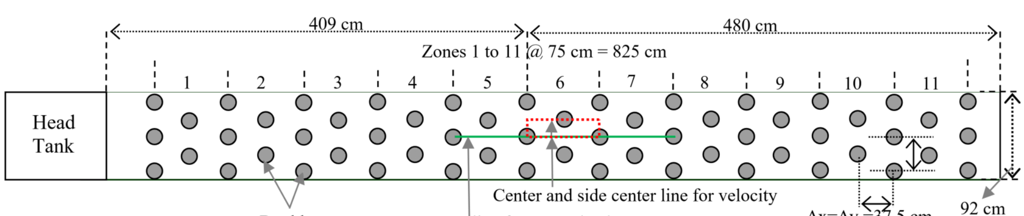

Figure 1: Plan view of the experimental setup of rock-ramp type fishpass (Baki et al. 2014a).

2.1.1 Mesh independence

Mesh resolution plays an important role in the modeling process since it has a significant effect on the accuracy of simulating velocity and water surface elevations. Ghamry and Katopodis (2017) performed several simulations to explore how mesh resolution affects model performance. The authors argue that applying finer resolution beyond an optimal mesh spacing may eventually reduce the accuracy rate improvement of the hydraulic model. In this sense, to investigate the mesh resolution effect in the model predictions and supporting the choice for the best mesh size, seven mesh resolutions were tested by comparing the simulated velocities and water depths with the observed ones in the Baki et al. (2014) experiment. Table 1 summarizes the main characteristics for each mesh, including the node spacing (size), the number of nodes and the number of triangle elements.

Table 1: Mesh characteristics

Characteristic	Mesh 1	Mesh 2	Mesh 3	Mesh 4	Mesh 5	Mesh 6	Mesh 7
Size (cm)	2.5	4	5	8	10	15	20
Number of nodes	12955	6613	5055	2600	1477	656	468
Number of elements	25243	12580	9631	4813	2682	1106	784

Three goodness-of-fit measures were used to check model fit to the experimental data: ((1) Mean Absolute Percentage Error (MAPE); (2) Root Mean Square Error (RMSE); and (3) the Coefficient of Determination (R^2); and their statistics are discussed later in Section 3.

[1] $\mathrm{MAPE} = \frac{1}{\mathrm{N}}\sum_{\mathrm{i=1}}^{\mathrm{N}}\left|\frac{\mathrm{X_{obs,i}}-\mathrm{X}_{sim,\mathrm{i}}}{\mathrm{X_{obs,i}}}\right| \times 100$

[2] $\mathrm{RMSE} = \sqrt{\frac{1}{\mathrm{N}}\sum_{\mathrm{i=1}}^{\mathrm{N}}(\mathrm{x_{obs,i}} - \mathrm{x_{sim,i}})^2}$

where, N is the number of observations (data), X_{obs} represents the observed or experimental data (velocity or hydraulic depth), and X_{sim} refers to the simulated values (velocity or hydraulic depth).

2.1.2 Model calibration

The model was calibrated by varying the effective roughness height (k_s) and the eddy viscosity coefficients (ε_1, ε_2, and ε_3) until a good agreement was obtained between the measured and simulated water levels and velocity. Three different bed roughness values including 0.0008 m, 0.0015 m and 0.0030 m were used to observe the performance of model in calculation of velocity and water depth. Different bed roughness values were chosen based on varying Manning's coefficients for a smooth steel bed (Chow 1959). The bed and side shear stresses of the Saint-Venant equations in River2D model arise primarily from turbulent flow interactions and are the corresponding friction slopes and the components of the turbulent stress respectively (Steffler and Blackburn 2002). Typically, friction slope terms depend on the bed shear stresses

[3] $S_{fx} = \frac{\tau_{bx}}{\rho g H} = \frac{u\sqrt{u^2+v^2}}{gHC_s^2}$

The Chezy coefficient is related to the effective roughness height, k_s, of the boundary, and the depth of flow through

[4] $C_s = 5.75 log\left(12\frac{H}{k_s}\right)$

where H is the water depth, u and v are the time averaged velocity in the longitudinal and transverse directions, τ_{bx} is the bed shear stress in the x-direction, ρ is water density, and g is the acceleration due to gravity.

Depth-averaged transverse turbulent shear stresses are modeled with a Boussinesq type eddy viscosity formulation:

[6] $\tau_{xy} = \vartheta_t \left(\frac{du}{dy} + \frac{dv}{dx}\right)$

where, ϑ_t is eddy viscosity coefficient. The eddy viscosity coefficient is assumed to be composed of three components: a constant (ε_1), a bed shear generated term with a factor of ε_2, and a transverse shear generated term with a factor of ε_3. Four runs with different combinations of eddy viscosity coefficients as shown in Table 2 were considered to examine the effect of these parameters on results as calibration parameters.

Table 2: Designed runs for different eddy viscosity coefficients as a calibration parameter

Run #	ε_1	ε_2	ε_3
1	0	0.5	0
2	0.05	0.5	0
3	0	0.7	0
4	0	0.5	0.05

3 RESULTS AND DISCUSSION

3.1 Optimal mesh discretization

To investigate how velocities and water surface elevation change depending on the mesh resolution, the simulations were compared with the experimental observations in zone 6 (center and side center lines) for velocity and zones 5 to 7 (center line) for water depth (Figure 1). Figure 2 presents a comparison between observed and simulated water surface profiles along the channel center lines between zones 5 and 7 under 60 L/s for different mesh sizes. The observed water surface profile has 4 valleys; however, except for the most refined mesh (2.5 cm) simulation, the others could basically represent only two valleys trend of the measured profile. Even though the 2.5 cm mesh simulation could capture the four valleys trend along the water surface profile, the level of accuracy with the observed trial was weak, overestimating the water level along almost all points and mismatching the last valley position. The simulations for 4, 5, 8, and 10 cm mesh generated valleys deeper than the measured ones while overestimated the water depth for the other points. On the other hand, simulations for mesh sizes 15 and 20 cm (coarser meshes) underestimated the water depth in almost all positions.

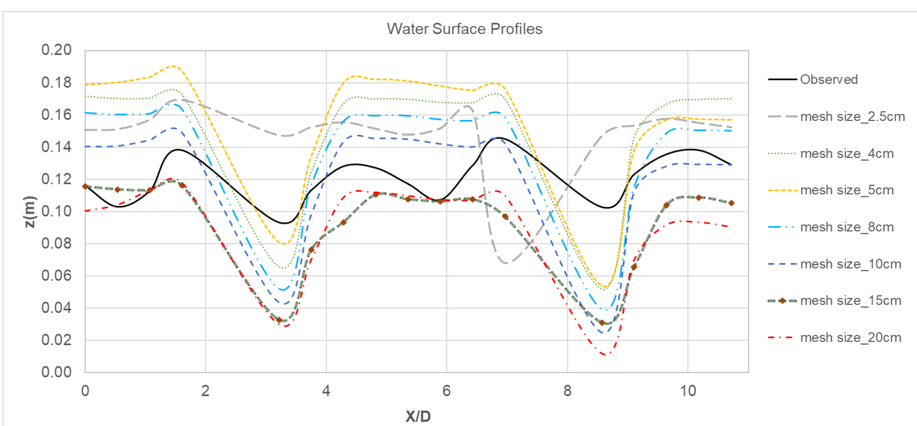

Figure 2: Observed and simulated water depth at 60 L/s for different mesh sizes in zones 5-7.

Figures 3 and 4 show the depth averaged velocity for the measurements (filled circled black dots) and for the simulations with different mesh sizes considering the center line and the side center line at 60 L/s. Visually, it is possible to identify that although the 2.5 cm mesh size simulation mismatch the measurements, it can reproduce the general behavior of the observed velocity profile more accurately when compared with the others mesh sizes.

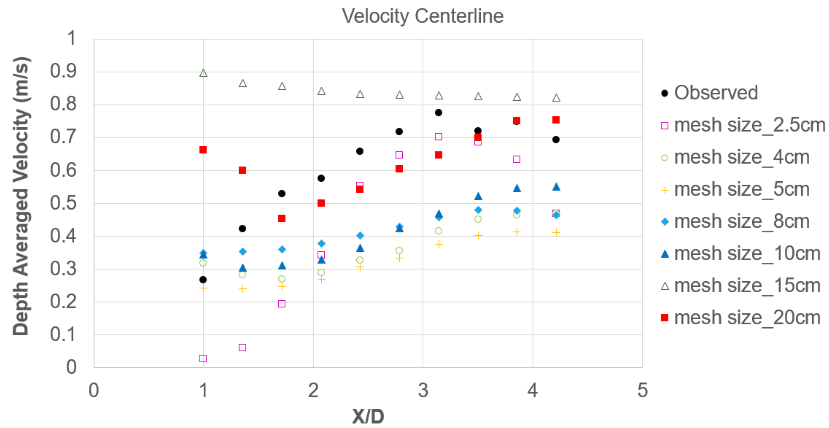

Figure 3: Observed and simulated depth averaged velocity for different mesh sizes in zone 6.

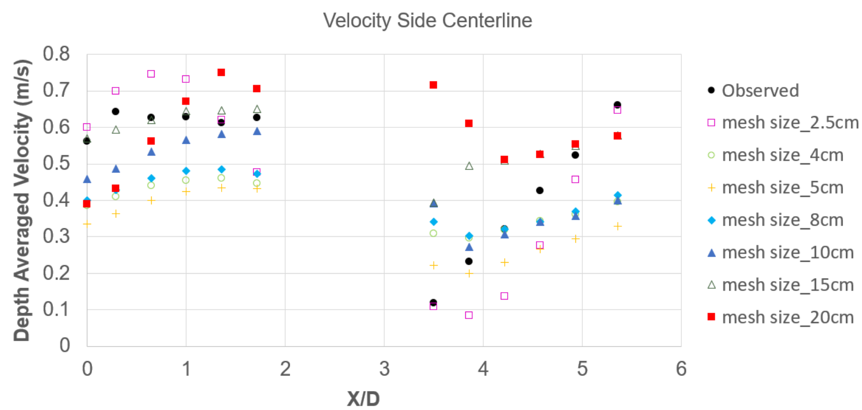

Figure 4: Observed and simulated depth averaged velocity for different mesh sizes in zone 6.

Figures 5 to 7 show that for the water depth, MAPE and RMSE indicate that the 10 cm mesh had the best performance. Refining the mesh size from 20 cm until 10 cm represented an improvement of MAPE and RMSE metrics; however, after refining the mesh smaller than 10 cm, reducing the mesh size made the results less accurate. Considering the R^2 metric a specific pattern was unclear and the optimal value obtained for mesh size was 4 cm.

Regarding the depth averaged velocity for the side center line, Figures 5 to 7 show a total agreement among the metrics in pointing out the most refined mesh (2.5 cm) as the mesh that better reproduced the observed values. On the other hand, for the center line, RMSE and MAPE indicates that the coarse mesh (20 cm) had the best agreement, while R^2 shows the 2.5 cm mesh with the highest agreement.

In this way, it is possible to infer that the best mesh resolution for simulations of water surface elevation will not always be the same for representing velocities profiles. In addition, for this case study, there was not a general behavior that allowed a script to define the optimal mesh resolution.

3.2 Model calibration

As mentioned earlier the model was calibrated using two parameters, effective roughness height (k_s) and the eddy viscosity coefficients (ε_1, ε_2, and ε_3). Firstly, the effect of three different k_s (0.0008m, 0.0015m, 0.003m) was observed to find a good agreement between the observations and numerical simulations.

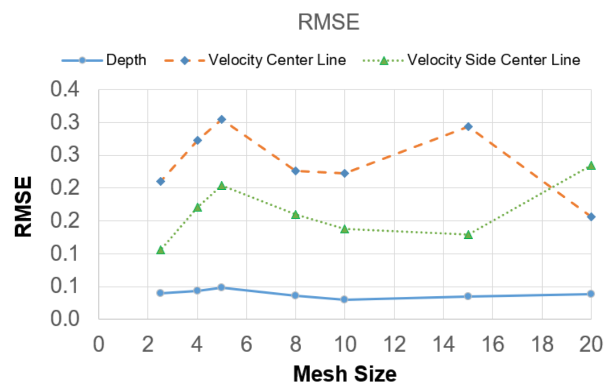

Figure 5: RMSE for the simulated depth and velocity for different mesh sizes at 60 L/s flow rate.

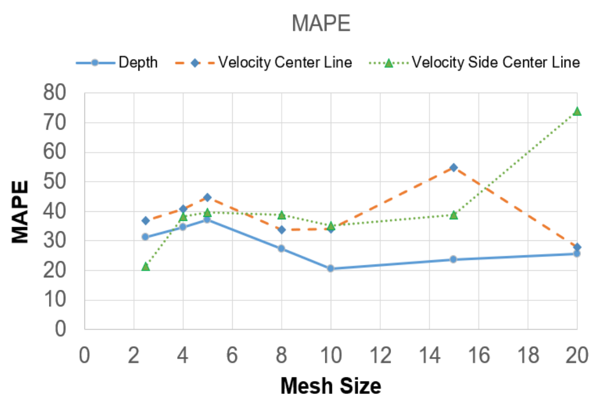

Figure 6: MAPE for the simulated depth and velocity for different mesh sizes at 60 L/s flow rate.

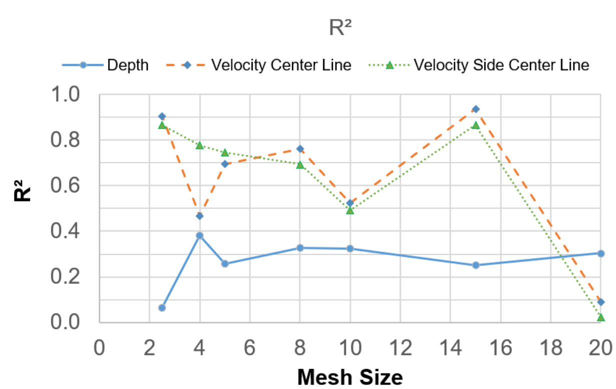

Figure 7: R^2 value for the simulated depth and velocity for different mesh sizes at 60 L/s flow rate.

Herein, randomly mesh size 5 cm was selected, as the model predictions are much more sensitive to the mesh resolution than to the bed roughness (Ghamry and Ktopodis 2017). Figure 8 (a) and (b) show RMSE and MAPE against varying bed roughness for depth and velocity along the channel center line and side center line, respectively, at flow rate 60 L/s. It can be found that there is not a specific trend between k_s and goodness-of-fit measures (RMSE and MAPE). Moreover, the different k_s lead to slight difference in errors. Therefore, the roughness height was not changed and k_s = 0.0008m was selected for further analysis.

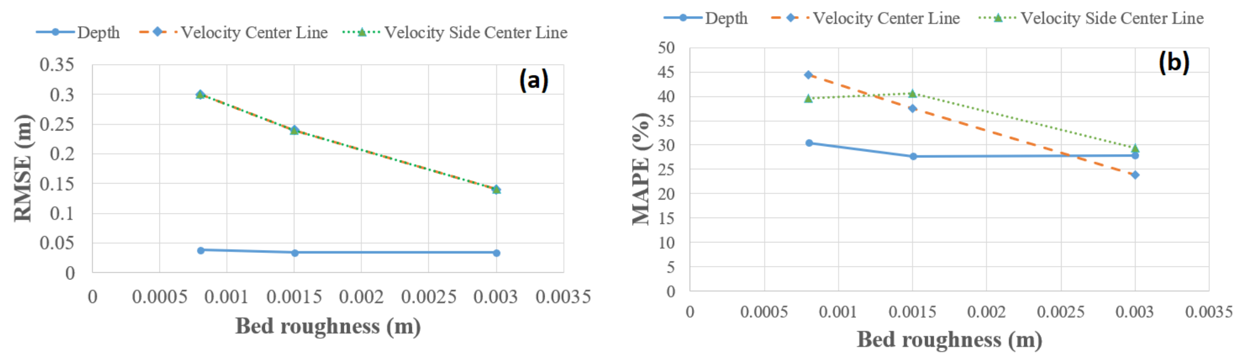

Figure 8: RMSE and MAPE value for the simulated depth and velocity at 60 L/s for 5cm mesh.

The next step of calibration was using different eddy viscosity coefficients. Table 3 shows the goodness-of-fit measures (RMSE, MAPE and coefficient of determination) for depth, velocity at center line and velocity at side center line along the measurement zone for different runs (i.e. different ε_1, ε_2, and ε_3) respectively. Figures 10 and 11 illustrate the changes of simulated depth and velocities for different runs. For the best resolution, all the runs were conducted for 2.5 cm mesh size and at 60 L/s flow rate. It can be found from the table and figures that there is no significant difference between run 1, run 3 and run 4. However, run 3 and run 4 show slight overall improvement. For run 2, a significant improvement can be observed. For instance, the coefficient of determination has been changed from 0.06 for run 1 to 0.47 for run 2. In addition, all the goodness-of-fit measures for run 2 show better performance in comparison with the other runs. Although in some case this improvement is not large, it shows an improving trend. Due to the shallow depth of this experiment, it is not surprising that slight changes of ε_1 improves the quality of results.

Table 3: Goodness-of-fit measures for simulated depth and velocities using different eddy viscosity coefficients for 2.5 cm mesh size at 60 L/s flow rate along the measurement zone

	Center line Depth			Center line velocity			Side center line velocity		
RUN#	RMSE	MAPE	R2	RMSE	MAPE	R2	RMSE	MAPE	R2
1	0.04	31.33	0.06	0.21	36.78	0.91	0.11	21.28	0.87
2	0.04	27.50	0.47	0.17	29.61	0.91	0.10	17.55	0.86
3	0.04	31.29	0.07	0.20	34.41	0.91	0.10	18.81	0.88
4	0.04	31.59	0.06	0.19	34.32	0.93	0.08	20.34	0.93

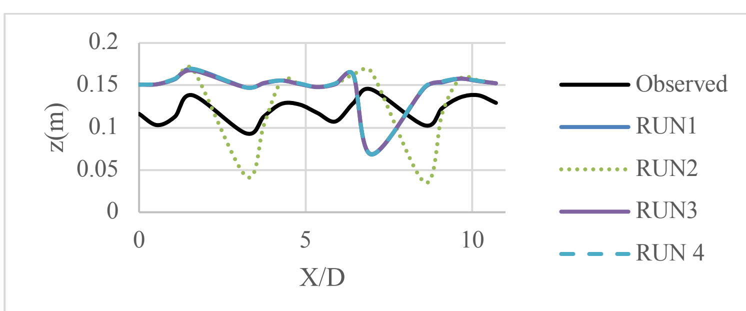

Figure 9: Observed and simulated water depth using different eddy viscosity coefficients for 2.5 cm mesh at 60 L/s flow rate in zones 5-7.

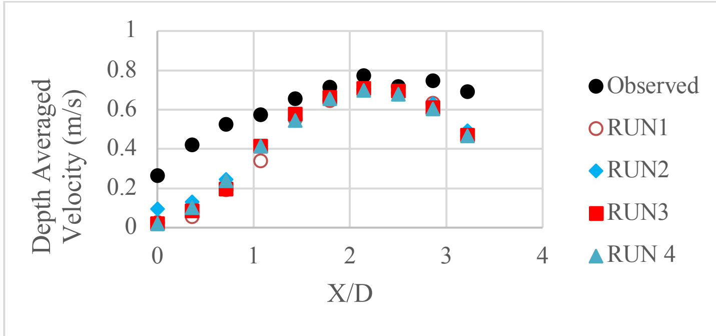

Figure 10: Observed and simulated velocity (center line) using different eddy viscosity coefficients for 2.5cm mesh at 60 L/s flow rate in zone 6.

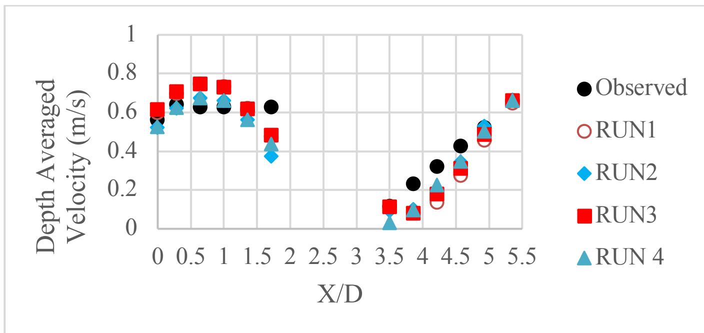

Figure 11: Observed and simulated velocity (side center line) using different eddy viscosity coefficients for 2.5 cm mesh at 60 L/s flow rate in zone 6.

4 CONCLUSIONS

This study determine the ability of River2D to model the flow through rock-ramp type nature-like fish pass by comparing the fish pass hydraulics (e.g., depth and velocity) between experimental measurements and numerical simulations. The results of mesh optimization suggest that the best mesh resolution for simulations of water surface elevation will not always be the same for representing velocities profiles. The 10 cm mesh had the best performance for the water depth, on the other hand 2.5 cm mesh had the best performance for the flow velocity. As expected, the roughness height (k_s) is less sensitive to the model predictions for depth and velocity. For the shallow water flow, the eddy viscosity coefficient ε_1 is more delicate than ε_2, and ε_3 to improve the reproduction of fishpass hydraulics. Considering water depth and velocity are one of the main criteria used for fishway design, it is expected that River2D model can help the designer of the NLF with caution. Further investigations are recommended to verify the ability of a 2D code (River2D) to model flow fields through fish pass.

5 REFERENCES

Clay, C.H. 1995. Design of Fishways and Other Fish Facilities, 2nd ed., Boca Raton, FL, USA.

Baki, A.B.M., Zhu, D.Z., Harwood, A., Lewis, A. and Healey, K. 2017a. Rock-weir fishway I: flow regimes and hydraulic characteristics. *Journal of Ecohydraulics*, **2**(2): 122-141.

Baki, A.B.M., Zhu, D.Z., Harwood, A., Lewis, A. and Healey, K. 2017b. Rock-weir fishway II: flow regimes and hydraulic characteristics. *Journal of Ecohydraulics*, **2**(2): 142-152.

Baki, A.B. M, Zhu, D.Z. and Rajaratnam, N. 2014a. Mean Flow Characteristics in a Rock-Ramp-Type Fish Pass. *Journal of Hydraulic Engineering*, **140**(2):156–68.

Baki, A.B., Zhu, D.Z. and Rajaratnam, N. 2014b. Turbulence Characteristics in a Rock-Ramp-Type Fish Pass. *Journal of Hydraulic Engineering*, **141**(2):156-158.
Baki, A.B.M., Zhu, D.Z. and Rajaratnam, N. 2016. Flow Simulation in a Rock-Ramp Fish Pass. *Journal of Hydraulic Engineering,* **142**(10): 4016031.
Brett, J.R. 1965. The Relation of Size to Rate of Oxygen Consumption and Sustained Swimming Speed of Sockeye Salmon (Oncorhynchus Nerka). *Journal of the Fisheries Board of Canada,* **22**(6):1491–1501.
Chow, V.T. 1959. *Open-Channel Hydraulics*. McGraw-Hill: New York, NY, USA.
Ghamry, H. and Katopodis, C. (2017). Computational optimization in simulating velocities and water surface elevations for habitat-flow functions in low-slope rivers. *Journal of Ecohydraulics,* **2**(2):99–121.
Hinch, S.G. and B.J. 2000. Effects of swim speed and activity pattern on success of adult sockeye salmon migration through an area of difficult passage. *Transactions of the American Fisheries Society* **129**(2): 598–606.
Jones, D.R., Kiceniuk, J.W. and Bamford O.S. 1974. Evaluation of the swimming performance of several fish species from the Mackenzie River. *Journal of the Fisheries Board of Canada,* **31**(10): 1641–47.
Katopodis, C.J., Kells, J.A. and Acharya, M. 2001. Nature-like and conventional fishways: Alternative concepts? *Canadian Water Resources Journal*, **26**(2): 211-32.
Kim, J.H., Yoon, J.D., Baek, S.H., Park, S.H., Lee, J.,W., Lee, J.A. and Jang, M.H. 2016. An efficiency analysis of a nature-like fishway for freshwater fish ascending a large Korean river. *Water,* **8**(1): 3.
Noonan,M.J., Grant, J.W.A. and Jackson, C.D. 2012. A quantitative assessment of fish passage dfficiency. *Fish and Fisheries*, **13**(14): 450-64.
Puertas, J., Cea, L., Bermúdez, M., Pena, L., Rodríguez, A., Rabuñal, J.R., Balairón, L., Lara, A. and Aramburu, E. 2012. Computer application for the analysis and design of vertical slot fishways in accordance with the requirements of the target species. *Journal of Ecological Engineering*, **48**(1): 51-60.
Peter, A., Bammatter, L., Mettler R. and Schölzel, N. 2017. Evaluation of the effectiveness of upstream fish passage facilities in the Rhine River assessed by a PIT-tagging study. *International Conference on Engineering and Ecohydrology for Fish Passage*, Oregon State University, Oregon, USA.
Roscoe, D.W. and Hinch, S.G. 2010. Effectiveness monitoring of fish passage facilities: Historical trends, geographic patterns and future directions. *Fish and Fisheries,* **11**(1):12–33.
Sfakiotakis, M., Lane, D.M., and Davies J.B.C. 1999. Review of fish swimming modes for aquatic locomotion. *IEEE Journal of Oceanic Engineering,* **24**(2): 237–52.
Steffler, P. and Blackburn, J. 2002. *Two-Dimensional Depth Averaged Model of River Hydrodynamics and Fish Habitat: Introduction to Depth Averaged Modeling and User's Manual*, Edmonton, Alberta, Canada, available from http://www.river2d.ualberta.ca/Downloads/documentation/River2D.pdf